Journal of Engineering Science and Technology
Vol. 16, No. 4 (2021) 3185 – 3198

BUBBLE COALESCENCE MODEL EFFECT ON OXYGEN MASS TRANSFER USING NON-NEWTONIAN FLUIDS

LILIBETH NIÑO[1], MARIANA PEÑUELA[1], GERMAN GELVES[2,*]

[1]Department of Chemical Engineering, Universidad de Antioquia,
Cll 67 No. 53-108, Medellín, Colombia
[2]Department of Environment, Universidad Francisco de Paula Santander,
Av. Gran Colombia No. 12E-96, Cúcuta, Colombia
*Corresponding Author: germanricardogz@ufps.edu.co

Abstract

A modified bubble coalescence model including rheological conditions and shear forces in non-Newtonian fluids is evaluated using CFD (Computational Fluid Dynamics). Euler's model, along with population balance equations, was used to simulate bubble size distribution. Simultaneously, different bubble breakage and coalescence models were evaluated to investigate mass transfer and bubble diameter. A conventional aeration stirring system (Rushton turbine, ring sparger) was used and the results were validated by determining the experimental mass transfer coefficient. A 10-liter bioreactor operated under different operating conditions commonly used for non-Newtonian rheology was used. Xanthan Gum 0.25% was used to resemble the rheological conditions developed during fungal culture. CFD results were contrasted with tested data obtained from $k_L a$ measurements at different stirring speeds using the concordance d-index. A reasonable prediction was obtained comparing the modified model Luo-New to the most used conventional models Luo-Luo and Laakkonen-Luo. Therefore, model Luo-New shows the highest d values at 400-700 rpm with values of 0.83, 0.95, 0.98 and 0.69. By contrast, the model Luo-Luo showed less inaccurate values with levels lower than 0.62 in almost all comparisons. The latter concludes numerically that the inclusion of viscosity effects and shear on a bubble coalescence model improves the degree of prediction related to oxygen transfer. The latter being a critical factor in the design and testing of stirring and aeration devices.

Keywords: Break up, Coalescence, Coulaloglou, Non-Newtonian fluids.

1. Introduction

Oxygen is required in many biochemical pathways. It is essential as a final electron acceptor in bioprocess reactions. However, in a stirred tank reactor, it is transferred into biological cells as dissolved oxygen, and due to its low solubility, the mass transfer rate is a challenge in bioreactor engineering technology.

Mycelia cultures behave as a non-Newtonian fluid in a stirred tank bioreactor. The latter affects oxygen transfer and leads to a depletion process. Computational Simulation focused on hydrodynamics studies allows for evaluating gas-liquid transport since bubble breakup and coalescence models are considered.

Mixing and oxygen transfer rate together are critical factors in industrial gas-liquid processes [1-3]. Therefore, oxygen transfer results from the bubble-fluid interaction. It is here that hydrodynamics simulation takes place since it simulates its effects on bubble breakup and coalescence. In such a way, CFD has been used to study stirred tanks, considering single rotating fluids [4-8] to use particle fluid interactions [9-15].

There are currently several coalescence models to simulate the bubble interaction with gas-liquid hydrodynamics [16]. However, the accuracy of these expressions is poorly studied in stirred tank bioreactors for non-Newtonian fluid applications. That is why the main objective of this research is to evaluate different coalescence models to determine their effects on mass oxygen transfer and its comparison with experimental data.

2. Bubble Breakup and Coalescence Models

Several authors [17-22] have developed different bubble breakup and coalescence models. However, reports are scarce regarding non-Newtonian fluids. Even so, some of the few studies [23-25] related to non-Newtonian liquids, using a different type of bioreactors considering several limitations.

That is why models proposed by [18] and [23] are evaluated as an initial point at this research. In addition to the above, a modified coalescence model is proposed that includes the shear rate as the main viscosity effect on non-Newtonian fluids. Its prediction capacity is evaluated together with those mentioned.

Considering turbulence, bubble breakage is caused by turbulent kinetic energy. A variety of models have been applied, based on critical values as critical turbulent kinetic energy [18-26], critical inertial force [20-21] and critical velocity fluctuations [27]. However, models are also developed in combination with other bubble coalescence expressions [18, 23]. This turbulent bombarding cascade of eddies increases the bubble surface energy until a critical value for causing the breakage. The bubble breakage rate is defined as [28]:

$$g(v')\beta(v|v') = k\int_{\xi_{min}}^{1} \frac{(1+\xi)^2}{\xi^{11/3}} exp\left(-b\xi^{-11/3}\right) d\xi \quad (1)$$

$$k = 0.9238\varepsilon^{1/3}d^{-2/3}\alpha \quad (2)$$

$$b = 12\left(f^{2/3+}(1-f)^{2/3}-1\right)\sigma\rho^{-1}\varepsilon^{-2/3}d^{-5/3} \quad (3)$$

Here d is the bubble size, ξ is the dimensionless eddy size, f means the breakup frequency, σ accounts for surface tension and α is named the air volume fraction. The breakup model [18] has been tested in this research to calculate its accuracy based on $k_L a$ mass transfer.

The bubble breaking model [23] is also used to describe the bubble breakup phenomenon in non-Newtonian fluids. It is expressed as the product between the breakup frequency (V') and $\beta[V,V']$ is the bubble distribution daughters:

$$(V') = c_2 \varepsilon^{1/3} erfc \sqrt{c_3 \frac{\sigma}{\rho_L \varepsilon^{2/3} d^{5/3}} + c_4 \frac{\mu_L}{\sqrt{\rho_L \rho_G \varepsilon^{2/3} d^{5/3}}}} \quad (4)$$

$$\beta(V,V') = \frac{30}{V'} \left(\frac{V}{V'}\right)^2 \left(1 - \frac{V}{V'}\right)^2 \quad (5)$$

Considering its previous applicability in non-Newtonian fluids, the breakup model [23] offers an alternative to breakage modelling [18]. That is why the models named here were selected to analyse their precision in bubble size determination.

Bubble coalescence is modelled considering bubble collision due to turbulence, buoyancy and laminar cut. The coalescence rate is defined as the product between the collision frequency $\omega_{ag}(v_i, v_j)$ and the coalescence efficiency $P_{ag}(v_i, v_j)$ and is defined as [28]:

$$a(v,v') = \omega_{ag}(v_i, v_j) P_{ag}(v_i, v_j) \quad (6)$$

The collision frequency is defined as:

$$\omega_{ag}(v_i, v_j) = c_{1,c} \ \frac{\pi}{4} \varepsilon^{\frac{1}{3}} (d_i + d_j)^2 \left(d_i^{\frac{2}{3}} + d_j^{\frac{2}{3}}\right)^{1/3} \quad (7)$$

where $c_{1,c}$ is a collision frequency constant between two particles with diameter d_i and d_j. The coalescence probability proposed by the Luo model [18] is expressed as:

$$P_C = exp\left[-c_e \frac{[0.75[1+\xi_{ij}^2][1+\xi_{ij}^3]^{1/2}]}{[\frac{\rho_g}{\rho_l}+\gamma][1+\xi_{ij}]^3} We_{ij}^{1/2}\right] \quad (8)$$

where c_e is a first-order constant, ρ_l and ρ_g are the densities of the primary (Gum xanthan) and secondary (air) phases. Eqs. (7) and (8) are the basis of the coalescence model proposed by [18] and it is used in this investigation as a reference point in combination with the breakup models mentioned in Table 1.

In addition to the breakup model [18], this research proposes a modified model for simulating coalescence, considering the shear rate effects on non-Newtonian fluids. So, Eq. (6) can be reformulated as follows:

$$a(v,v') = \omega_{cT}(v_i, v_j) P_{cT}(v_i, v_j) + \omega_{c\dot{\gamma}}(v_i, v_j) P_{c\dot{\gamma}}(v_i, v_j) \quad (9)$$

Here $\omega_{cT}(v_i, v_j)$ is the coalescence frequency due to turbulent kinetic energy reached in a stirred tank, $P_{c\dot{\gamma}}(v_i, v_j)$ calculates the coalescence probability, $\omega_{c\dot{\gamma}}(v_i, v_j)$ is the coalescence frequency due to the shear rate and $P_{c\dot{\gamma}}(v_i, v_j)$ refers to the probability of the coalescence triggered by the shear rate $\dot{\gamma}$.

The collision rate $\omega_{cT}(v_i, v_j)$ resulting from turbulence is expressed as [16]:

$$\omega_{cT}(v_i, v_j) = \frac{c_{c,1} \varepsilon^{1/3} (d_i + d_j)^2}{(1+\emptyset)} \left(d_i^{2/3} + d_j^{2/3}\right)^{1/2} \quad (10)$$

The coalescence probability $P_{cT}(v_i, v_j)$ can be related to coalescence and contact time reached a stirred tank bioreactor. Therefore, force compressing bubbles must be sufficient, so that thinning film covering bubbles needs to be drained to a critical value, thus triggering the coalescence [29], resulting:

$$P_{cT}(v_i, v_j) = exp\left(-c_{c,2}\frac{\mu_L \rho_L \varepsilon}{\sigma^2(1+\emptyset)^3}\left(\frac{d_i d_j}{d_i + d_j}\right)^4\right) \quad (11)$$

In a turbulent field, Bubbles, dominated by a circular flow pattern, can coalesce to lead larger bubbles. Shear rate impacts on bubble coalescence can be modelled according to [30]:

$$\omega_{c\dot{\gamma}}(v_i, v_j) = \frac{4}{3}\left(\frac{d_i + d_j}{2}\right)^3 \left(\frac{\mu_{ap}}{K}\right)^{\frac{1}{n-1}} \quad (12)$$

K and n are parameters for the viscosity power-law model. Viscosity acts as a resistance force to fluid deformation and also depends considerably on the shear rate. Based on the latter, this resistance to fluid flow is overcome by the shear rate. Consequently, the viscosity will be high in less mixed zones and high bubble coalescence will be evident.

Shear rate impacts on bubble coalescence are calculating using Eq. (12). Based on previous experiments [31, 32], bubble size distribution on shear impacts can be represented as an empirical expression. That is why, in this research, the following exponential term:

$$P_{c\dot{\gamma}}(v_i, v_j) = exp^{-\frac{\left(\frac{\mu_{ap}}{K}\right)^{\frac{1}{n-1}}}{A,c}} \quad (13)$$

Equations (9) to (13) constitute the modified coalescence model used in this research.

The main objective during the comparison of the proposed models was to determine the accuracy of the bubble breakup-coalescence model that allows covering a wide range of physical properties, operating conditions, and in turn, applicable from the point of view of hydrodynamic analysis. For the study of the breakup and coalescence phenomena, the following models were selected:

Table 1. Bubble Breakup-Coalescence models evaluated.

Cases	Combination Kernel	Model
Case 1:Luo-Inv	Luo and Svendsen [18] Luo-New	Breakup Coalescence
Case 2:Luo-Luo	Laakkonen [23] Luo and Svendsen [18]	Break-up Coalescence
Case 3: Laak-Inv	Laakkonen [23] Luo-New	Break-up Coalescence
Case 4:Laak-Luo	Laakkonen [23] Luo and Svendsen [18]	Break-up Coalescence

3. Stirred Tank Physical Characteristics and Experiments

For modelling in CFD and experiments, a New Brunswick stirred tank bioreactor, as shown in Fig. 1 was used at a laboratory scale with 10 litres as work volume. The tank is characterized by the following dimensions: DT diameter: 0.21 m, liquid HL: 0.3 m, equipped with four deflectors spaced at an angle of 90° with a width Wb: 0.1DT installed at a distance of the walls of 0,010 m. The equipment has a 6-blade Rushton turbine impeller with a diameter Di: 0.075 m. Air is supplied through a sparger of 0.06 m in diameter.

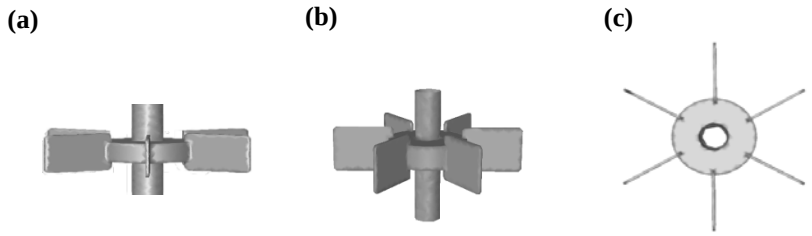

Fig. 1. Rushton turbine; (a) Front view, (b) Diagonal view, (c) Cross section.

Stirring set-ups are tested between 200-800 rpm and air flow was evaluated at 1.0 vvm based on commonly operational conditions for fungal applications. Previous research [33, 34] suggest mycelium cultures act as non-Newtonian fluid similar to the power-law viscosity model:

$$\mu_{appar} = K\gamma^{n-1} \quad (14)$$

Viscosity model constants were calculated experimentally and coupled to hydrodynamic modelling. Brookfield DV-E viscometer was used, applying shear rates at 1-100 s^{-1}. To validate the CFD model, the $k_L a$ values were determined experimentally at a 10-liter scale, using 0.25% Xanthan gum to simulate the rheological effects of a fungal culture at the bioreactor level. For the experimental $k_L a$ determination, the tank is gasified with nitrogen for removing dissolved oxygen [4]. Then the air is supplied and dissolved oxygen C_L is measured until saturation is reached using a DO sensor (InPro 6800, Mettler Toledo, Germany). The rate of change of oxygen is calculated using the following equation:

$$\frac{dC_L}{dt} = k_L a(C_L^* - C_L) \quad (15)$$

where C_L^* is the oxygen saturation level and C_L is the dissolved oxygen concentration. Solving the eq. (15) an expression for determining $k_L a$ results:

$$k_L a = \frac{1}{t}\left[\frac{C_L^* - C_L}{C_L^*}\right] \quad (16)$$

To quantify the degree of similarity regarding $k_L a$ experimental and simulated data, the concordance index d proposed by [35] is evaluated.

4. Results and Discussions

Different bubble breakup and coalescence models were evaluated mainly to investigate the mass transfer in a bioreactor stirred by a Rushton turbine. Results were assessed experimentally by determining the mass transfer coefficient $k_L a$. Xanthan Gum at 0.25% was used to resemble the rheological conditions developed during fungal culture [34, 36]. The oxygen transfer behaviour is observed experimentally under different stirring speeds and compared to data obtained from simulations shown in Fig. 2. Various scenarios are observed defined by each breakup and coalescence model evaluated. The latter suggests that $k_L a$ is significantly dependent on bubble interaction generated in a stirring-aeration system.

According to experimental data $k_L a$ (Fig. 2), it is observed for cases 3 (Laak-New) and 4 (Laak-Luo) a $k_L a$ sub-prediction regarding breakup and coalescence models at stirring levels greater than 600 rpm. However, mass transfer is overestimated at lower stirring values. This particularity is more noticeable in case 4

(Laak-Luo), in which the coalescence rate defined by [18] was used. In comparison with the other studies, it is observed that $k_L a$ values mostly tend to be oversized at case 2 (Luo-Luo). Under these conditions, the Luo-Luo model results in the estimation of small bubbles. This latter implies that the breakup phenomenon mainly dominates bubble interaction. According to the results on this case, it is observed that this model combination [18] tends to increase the breakup rate. The coalescence model effect proposed in this investigation can be analysed according to results obtained from $k_L a$ values for case 1 (Luo-New) and case 3 (Laak-New). In such a way, it is observed a better accurate in Case 1 than all the evaluated models.

The model proposed by Laakkonen [23] in case 3 tends to decrease the breakage rate and therefore underestimates the $k_L a$ values. For this reason, the increase in bubble size results from the prevalence of coalescence phenomena, which can be observed in Figs. 3 and 4. The latter is one of the typical characteristics of non-Newtonian fluids. However, the model (Case 3) fails to predict that behaviour, since this model [23], combined with the coalescence phenomenon, captures the breakup phenomenon to a lesser extent than the evaluated model in Case 1.

The breakup Luo model [18], based on the gas kinetic theory, allows a better approximation of bubble breakup and coalescence phenomena in non-Newtonian fluids (Luo-New). The breakup Luo model [18] has been the basis of numerous modeling studies in Newtonian and non-Newtonian fluids [23, 37, 38]. So it has an advantage compared to the breakup Laakkonen model [23] since the daughter bubble distribution function can be calculated directly from the breakup model. The latter allows a lower computational time, while the Laakkonen break model [23] requires an additional function for the daughter bubble distribution.

It is possible to state that breakage rates prevail over coalescence rates, regarding case 2 [Luo-Luo]. The above-explained by the high $k_L a$ values and also the small bubble diameters calculated (Fig. 3). The latter indicates that the coalescence model proposed by Luo [18] does not take into account the shear rate effect on fluid bubble interaction. The latter is a significant phenomenon for mechanical design, which considers the rheology in a stirring-aeration system.

When comparing the coalescence model, it is observed the best prediction related to experimental and simulated $k_L a$ values in case 1 [Luo-New.]. The model proposed in this study includes the shear rate effect on bubble coalescence. That is why the breakup rate increases with increasing dissipation energy, mainly due to the stirring speed. The latter also induces an increase in bubble collision frequency and kinetic energy [39]. According to [37], bubble breakup and coalescence phenomena vary in mild turbulence conditions, such as non-Newtonian fluids.

In non-Newtonian fluids, the shear force τ depends on the rheological properties and stirring rate [40-46]. That is why this research proposes a modified semi-empirical model that considers the shear rate effect on bubble coalescence. The latter is an important phenomenon that must be taken into account during the design focuses on improving $k_L a$. In an aerobic fermentation, air flows continuously through the stirred tank reactor. For this reason, the bubble size distribution results from the interaction of physical mechanisms such as breakup and coalescence. The most important parameter to analyse these hydrodynamic mechanisms is the mean Sauter diameter [14].

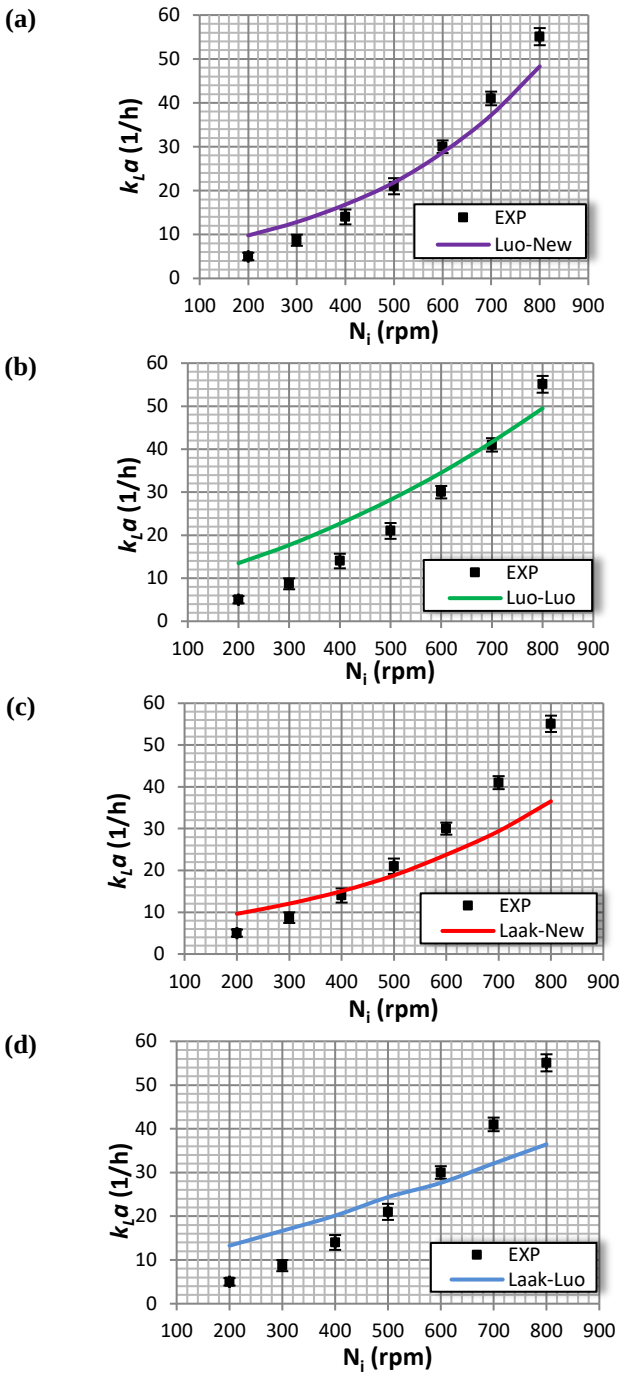

Fig. 2. k_La Determination at different stirring rates [EXP: Experimental data]. (a) Luo-New; (b) Luo-Luo; (c) Laak-New; (d) Laak-Luo.

This parameter is essential in Bioreactors' design since it is essential to understand the mechanism of oxygen mass transfer performance through bubble behaviour. Bubble diameter was evaluated at different coalescence and breakup models. Figure 3 shows the behaviour of bubble diameter at different radial positions [r/R]. For case 2 [Luo-Luo], the model tends to increase the breakup rate. The bubble diameters are smaller [<4.5 mm] compared with the other models, resulting in high oxygen transfer values, as seen in Figs. 2 and 3.

Case 3 [Laak-New] shows high bubble diameters [> 5.5mm] at shaking speeds of 400, 600 and 800. This model tends to over-predict the bubble coalescence rate because larger bubble diameters are observed. Therefore, the breakup phenomenon is low in this combination of models. Case 4 [Laak-Luo] sub-predicts the diameter of the bubbles at 200 and 400 rpm [<5.5 mm]. Therefore, the model maximizes the breakup phenomenon, showing higher $k_L a$ values , while it over-estimates the bubble diameter [> 5.5mm], at 600 and 800 rpm maximizing the coalescence phenomenon and resulting in low $k_L a$ values. For case 1 [Luo-New], it is observed that the model calculates consistently the bubble diameter. As seen in Fig. 3, rheology effects influence the average bubble size. Coalescence phenomena predominate bubble dynamics in non-Newtonian fluids. According to [23], the dissipation energy decreases, and bubble size is large by increasing the liquid viscosity, resulting in a smaller interfacial area and therefore, the oxygen transfer decreases. In Fig. 3, it is observed that bubble diameter tends to be short at areas closed to the blade and large in the middle part of the bioreactor. That is, the $k_L a$ mass transfer is more significant near the area where the stirrer is located, due to more substantial bubble breakage. Turbulent energy originates mainly from the movement of the agitator. That is why turbulence controls the breakup and coalescence phenomena and hence mass transfer [23]. This behaviour is because the bubble size is dependent on turbulence scales and flow patterns. The latter, due to the relationship between the local energy dissipation rates, the bubble residence time, breakage and coalescence rates [2, 3].

To quantify the degree of similarity between the experimental data and the simulated data, the concordance index developed by Willmott et al. [35] was evaluated. The concordance indexes reflect the degree to which the observations' variance is estimated accurately by the prediction variance. Its range can vary between 0.0 and 1.0, where 1.0 indicates a perfect match between observations and simulated data.

In Fig. 5, the concordance indexes calculated for the experimental and simulated $k_L a$ data at different stirring rates are observed. It is observed a consistency related to the accuracy, according to the analysed observations. Figure 4 shows that cases 2 and 4 [Luo-Luo and Laak-Luo] present the lowest concordance rates for each stirring speed. For case 3 [Laak-New], it is observed that the concordance index was higher only at 400 rpm. The index was lower for other cases. Case 1 [Luo-New] shows the highest concordance values at all stirring speeds than the other models evaluated. At low velocities (200, 300 rpm), the concordance values are lower (0.39; 0.58). While at (400, 500, 600, 700 and 800 rpm) the concordance indexes are those that present the higher values (0.83; 0.95 and 0.98; 0.69 and 0.56). The above reveals the importance of including the shear velocity effect on bubble coalescence, as proposed in the new model described in this investigation.

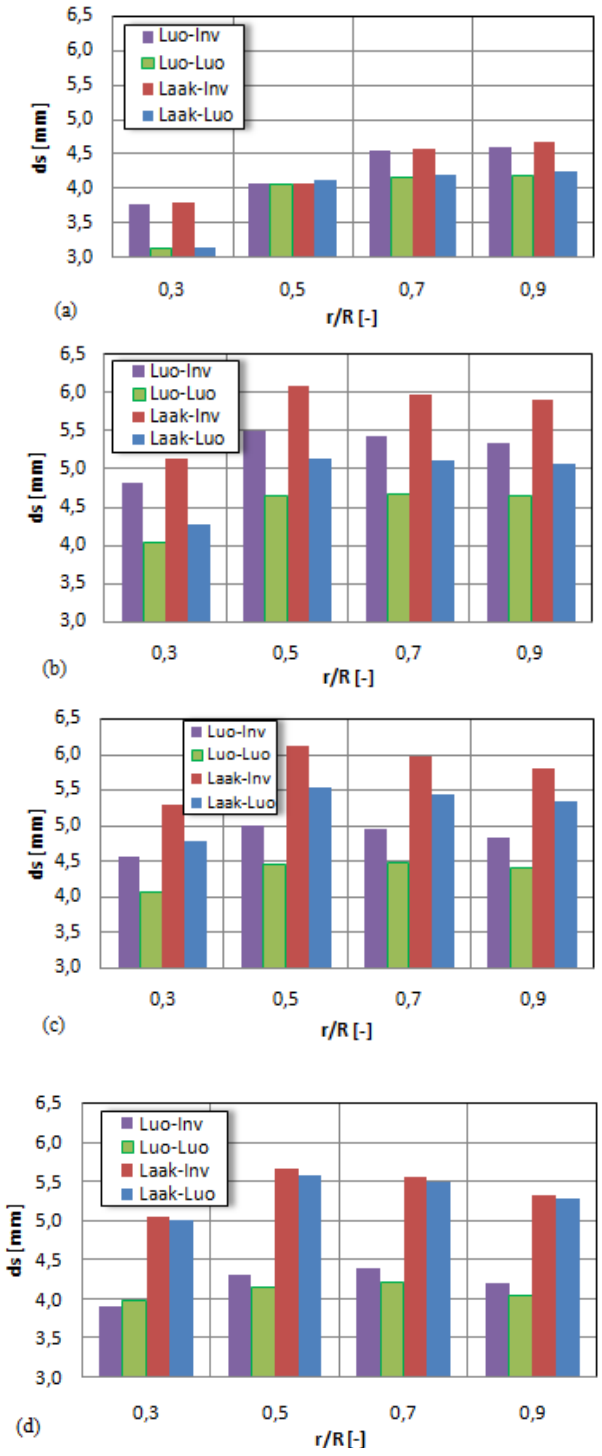

Fig. 3. Bubble diameter vs [r/R].
(a) 200 rpm, (b) 400 rpm, (c) 600 rpm and (d) 800 rpm.

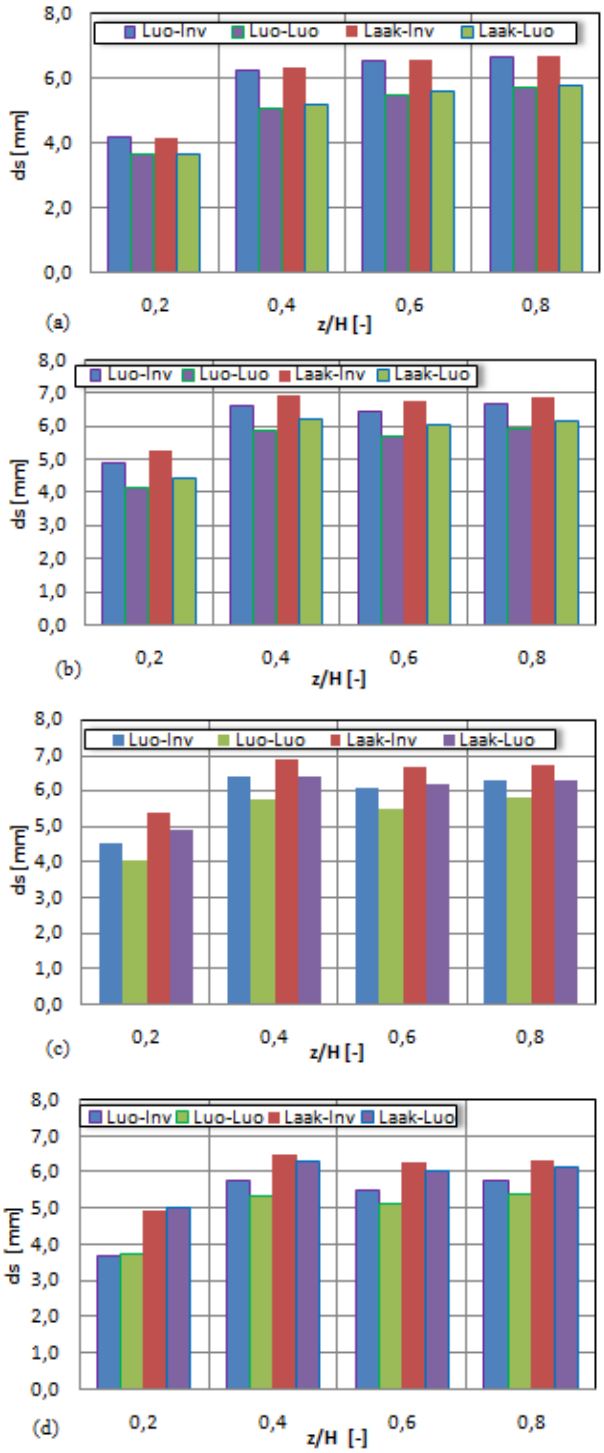

Fig. 4. Bubble diameter simulations at different stirring speeds and axial position [z / H], (a) 200 rpm, (b) 400 rpm, (c) 600 rpm and (d) 800 rpm.

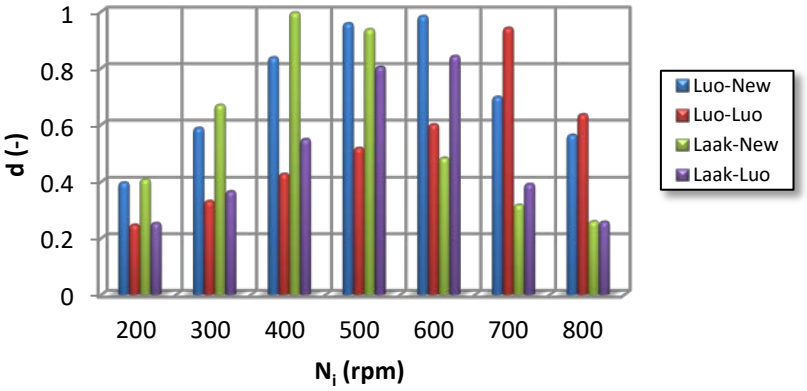

Fig. 5. Concordance indexes calculated for experimental and simulated $k_L a$ data.

The coalescence model proposed in this research allows an acceptable approximation based on experimental $k_L a$ data. It is important to highlight the applicability of this model since it allows the dissipation energy to be related to the shear rate effect on the influence of stirring speed. These parameters are of paramount importance in the improvement of stirring-aeration devices in non-Newtonian fluids.

5. Conclusions

In this study, a modified model based on the shear rate is proposed to capture coalescence and bubble breakup phenomena compared to experimental data. Based on the results, the modified model considerably increases accurate predictions. The latter showed the highest concordance index values calculating an acceptable approximation related to results obtained through simulations by CFD and the experimental $k_L a$ data. A significant effect of the shear rate was found. The latter also explained by the simulation of $k_L a$ and bubble sizes by demonstrating numerically that the inclusion of viscosity effects and shear on a bubble coalescence model improves the degree of prediction related to oxygen transfer.

References

1. Lehr, F.; Millies, M.; and Mewes, D. (2004). Bubble-size distributions and flow fields in bubble columns. *American Institute of Chemical Engineering*, 48(11), 2426-2443.
2. Karimi, A.; Golbabaei, F.; Mehrnia, M.R.; Neghab, M.; Mohammad, K.; Nikpey, A.; and Pourmand, M.R. (2013). Oxygen mass transfer in a stirred tank bioreactor using different impeller configurations for environmental purposes. *Iranian Journal of Environmental Health Science and Engineering*, 10(1), 1-6.
3. Amaral, P.F.F.; Freire, M.G.; Rocha-Leão, M.H.M.; Marrucho, I.M.; Coutinho, J.A.P.; and Coelho, M.A.Z. (2008). Optimization of oxygen mass transfer in a multiphase bioreactor with perfluorodecalin as a second liquid phase. *Biotechnology and Bioengineering*, 99(3), 588-598.

4. Nino, L.; Gelves, R.; Ali, H.; Solsvik, J.; and Jakobsen, H. (2020). Applicability of a modified breakage and coalescence model based on the complete turbulence spectrum concept for CFD simulation of gas-liquid mass transfer in a stirred tank reactor. *Chemical Engineering Science*, 211, 52-72.
5. Alopaeus, V.; Koskinen, J.; and Keskinen, K.I. (1999) Simulation of the population balances for liquid-liquid systems in a nonideal stirred tank. Part 1 description and qualitative validation of the model. *Chemical Engineering Science*, 54(24), 5887-5899.
6. Moilanen, P. (2009). *Modeling gas-liquid flow and local mass transfer in stirred tanks*. Doctoral dissertation, Helsinki University of Technology.
7. Jenne, M.; and Reuss, M. (1999). A critical assessment on the use of k-ε turbulence models for simulation of the turbulent liquid flow induced by Rushton turbine in baffled stirred-tank reactors. *Chemical Engineering Science*, 54(17), 3921-3941.
8. Luo, J.Y.; Issa, R.I.; and Gosman, A.D. (1994). Prediction of impeller induced flows in mixing vessels using multiple frames of reference. *Proceedings of the 8th European Conference on Mixing*. Cambridge, United Kingdom, 549-556.
9. Micale, G.; Brucato, A.; Grisafi, F.; and Ciofalo, M. (1999). Prediction of flow fields in a dual-impeller stirred vessel. *American Institute of Chemical Engineering*, 45(3), 445-464.
10. Tabor, G.; Gosman, A.D.; and Issa, R.I. (1996). Numerical simulation of the flow in a mixing vessel stirred by a Rushton turbine. *Institute of Chemical Engineering*, 32, 352-356.
11. Rutherford, K.; Lee, K.C.; Mahmoudi, S.M.S.; and Yianneskis, M. (1996) Hydrodynamic characteristics of dual Rushton impeller stirred vessels. *American Institute of Chemical Engineering*, 42(2), 332-346.
12. Bakker, A.; and Akker, H.E.A.V.D. (1994). A computational model for the gas-liquid flow in stirred reactors. *Chemical Engineering Research and Design*, 72(A4), 573-582.
13. Kerdouss, F.; Bannari, A.; Proulx, P.; Bannari, R.; Skrga, M.; and Labrecque, Y. (2008). Two-phase mass transfer coefficient prediction in a stirred vessel with a CFD model. *Computers and Chemical Engineering*, 32(8), 1943-1955.
14. Kerdouss, F.; Kiss, L.; Proulx, P.; Bilodeau, J.-F.; and Dupuis, C. (2005). Mixing characteristics of an axial-flow rotor: experimental and numerical study. *International Journal of Chemical Reactor Engineering*, 3(1).
15. Lane, G.L.; Schwarz, M.P.; and Evans, G.M. (2002). Predicting gas-liquid flow in a mechanically stirred tank. *Applied Mathematical Modelling*, 26(2), 223-235.
16. Solsvik, J.; and Jakobsen, H.A. (2015). A review of the statistical turbulence theory required extending the population balance closure models to the entire spectrum of turbulence. *American Institute of Chemical Engineering*, 62(5), 1795-1820.
17. Liao, Y.; and Lucas, D. (2010). A literature review on mechanisms and models for the coalescence process of fluid particles. *Chemical Engineering Science*, 65(10), 2851-2864.
18. Luo H.; and Svendsen, H.F. (1996). Theoretical model for drop and bubble break-up in turbulent dispersions. *American Institute of Chemical Engineering*, 42(5), 1225-1233.

19. Prince, M.J.; and Blanch, H.W. (1990). Bubble coalescence and breakup in air-sparged bubble columns. *American Institute of Chemical Engineering*, 36(10), 1485-1499.
20. Niño, L.; Gelves, R.; Ali, H.; Solsvik, J.; and Jakobsen, H. (2020). Applicability of a modified breakage and coalescence model based on the complete turbulence spectrum concept for CFD simulation of gas-liquid mass transfer in a stirred tank reactor. *Chemical Engineering Science*, 211, 115272.
21. Lehr, F.; and Mewes, M.M.D. (2004). Bubble-size distributions and flow fields in bubble columns. *American Institute of Chemical Engineering*, 48(11), 2426-2443.
22. Alopaeus, V.; Koskinen, J.; and Keskinen, K.I. (1999). Simulation of the population balances for liquid-liquid systems in a nonideal stirred tank. Part 1 description and qualitative validation of the model. *Chemical Engineering Science*, 54(24), 5887-5899.
23. Laakkonen, M. (2006). *Development and validation of mass transfer models for the design of agitated gas-liquid reactors*. Doctor dissertation, Helsinki University of Technology.
24. Moilanen, P. (2009). *Modeling gas-liquid flow and local mass transfer in stirred tanks*. Doctor dissertation, Helsinki University of Technology.
25. Han, M. (2017). Hydrodynamics and mass transfer in airlift bioreactors : experimental and numerical simulation analysis. Doctor dissertation, Lappeenranta University of Technology.
26. Chatzi, E.G.; Gavrielides, A.D.; and Kiparissides, C. (1989). Generalized model for prediction of the steady-state drop size distributions in batch stirred vessels. *Industrial Engineering of Chemical Research*, 28(11), 1704-1711.
27. Alopaeus, V.; Keskinen, K.I.; Koskinen, J.; and Majander, J. (2003). Gas-liquid and liquid-liquid system modeling using population balances for local mass transfer. *Computer Aided Chemical Engineering*, 14, 545-549.
28. Robertson, B.; and Ulbrecht, J.J. (1987). Measurement of shear rate on an agitator in a fermentation broth. *Proceedings of the Biotechnology Processes: Scale-up Mixing*. Miami, USA, 72-81.
29. Coulaloglou, C.A.; and Tavlarides, L.L. (1977). Description of interaction processes in agitated liquid-liquid dispersions. *Chemical Engineering Science*, 32(11), 1289-1297.
30. Jakobsen, H.A.; Lindborg, H.; and Dorao, C.A. (2005). Modeling of bubble column reactors: progress and limitations. *Industrial Engineering of Chemical Research*, 44(14), 5107-5151.
31. Sundararaj, U.; and Macosko, C.W. (1995). Drop breakup and coalescence in polymer blends: the effects of concentration and compatibilization. *Macromolecules*, 28(8), 2647-2657.
32. Terasaka, K.; Murata, S.; and Tsutsumino, K. (2008). Bubble distribution in shear flow of highly viscous liquids. *The Canadian Journal of Chemical Engineering*, 81(3-4), 470-475.
33. Chavez-Parga, M.C.; Gonzalez-Ortega, O.; Negrete-Rodriguez, M.L.X.; Medina-Torres, L.; and Silva, E.M.E. (2007). Hydrodynamics, mass transfer and rheological studies of gibberellic acid production in an airlift bioreactor. *World Journal of Microbiological Biotechnology*, 23(5), 615-623.

34. Gabelle J.-C.; Jourdier, E.; Licht, R.B.; Chaabane, F.B.; Henaut, I.; Morchain, J.; and Augier, F. (2012). Impact of rheology on the mass transfer coefficient during the growth phase of *Trichoderma reesei* in stirred bioreactors. *Chemical Engineering Science*, 75, 408-417.
35. Willmott, C.J.; Steven, G.A.; Davis, R.E.; Feddema, J.J.; Klink, K.M.; Legates, D.R.; O'Donnell, J.; and Rowe, C.M. (1985). Statistics for the evaluation and comparison of models. *Journal of Geophysical Research*, 90(5), 8995-9005.
36. Gelves, R.; Dietrich, A.; and Takors, R. (2014). Modeling of gas-liquid mass transfer in a stirred tank bioreactor agitated by a Rushton turbine or a new pitched blade impeller. *Bioprocess and Biosystems Engineering*, 37(3), 365-375.
37. Nino, L.; Peñuela, M.; and Gelves, G.R. (2018). Gas-liquid hydrodynamics simulation using CFD in a helical ribbon impeller applied for non-newtonian fluids. *International Journal of Applied Engineering Research*, 13(11), 9353-9359.
38. Politano, M.S.; Carrica, P.M.; and Balino, J.L. (2003). About bubble breakup models to predict bubble size distributions inhomogeneous flows. *Chemical Engineering Communications*, 190(3), 299-321.
39. Han, M.; Sha, Z.; Laari, A.; and Koiranen, T. (2017). CFD-PBM coupled simulation of an airlift reactor with non-newtonian fluid. *Oil & Gas Science and Technology*, 72(5), 1-12.
40. Hernandez, S.; Niño, L.; and Gelves, G. (2020). Simulating of Microbial Growth Scale Up in a Stirred Tank Bioreactor for Aerobic Processes using Computational Fluid Dynamics. *Journal of Physics: Conference Series*, 1655 1-6.
41. Chisti, Y.; and Moo-Young, M. (1989). On the calculation of shear rate and apparent viscosity in airlift and bubble column bioreactors. *Biotechnology and Bioengineering*, 34(11), 1391-1392.
42. Sanchez-Pérez, J.A.; Porcel, E.M.R.; López, J.L.C.; Sevilla, J.M.F.; and Chisti, Y. (2006). Shear rate in a stirred tank and bubble column bioreactors. *Chemical Engineering Journal*, 124(1-3), 1-5.
43. Gelves, G. (2020). Simulating hydrodynamics in a Rushton turbine at different stirring velocities applied to non-Newtonian fluids. *Proceedings of the 6th International Week of Science, Technology and Innovation*. San José de Cúcuta, Colombia, 1-7.
44. López, L.C.N.; Peñuela, M.; and Gelves, G. (2016). Improving of gas-liquid mass transfer in a stirred tank bioreactor: A CFD approach. *International Journal of Applied Engineering. Research*, 11(9), 6097-6108.
45. Niño-López, L.C.; and Gelves-Zambrano, G.R. (2015). Simulating gas-liquid mass transfer in a spin filter bioreactor. *Revista Facultad de Ingeniería*, 1, 163-174.
46. Niño-López, L.; Cárdenas, A.A.; and Zambrano, R.G. (2013). Evaluation of chemical pretreatments for enzymatic hydrolysis of lignocellulosic residues cassava (*Manihot esculenta Crantz). Revista Facultad de Ingeniería*, 69, 317-326.